http://www.scirp.org/journal/ns Natural Science, 2017, Vol. 9, (No. 10), pp: 355-376

Isotopes (^{13}C and ^{18}O) Geochemistry of Lower Triassic Montney Formation, Northeastern British Columbia, Western Canada

Edwin I. Egbobawaye

Department of Earth and Atmospheric Sciences, 1-26 Earth Sciences Building, University of Alberta, Edmonton, Canada

Correspondence to: Edwin I. Egbobawaye, Egbobawayeiii@gmail.com

Keywords: Isotopes, Stable Isotopes, ^{13}C and ^{18}O, Isotope Geochemistry, Montney Formation, Geochemistry, Chemical Element, Mineralogy, Tight Gas Reservoir, British Columbia, Western Canada Sedimentary Basin (WCSB), Triassic, Subsurface Geology

Received: December 3, 2016 **Accepted:** October 27, 2017 **Published:** October 30, 2017

ABSTRACT

Oxygen isotope ($\delta^{18}O$) serves as paleothermometer, and provides paleotemperature for carbonates. $\delta^{18}O$ signature was used to estimate the temperature of fractionation of dolomite and calcite in Montney Formation, empirically calculated to have precipitated, between approximately 13˚C to ±33˚C during Triassic time in northeastern British Columbia, Western Canada Sedimentary Basin (WCSB). Measurements of stable isotopes ($\delta^{13}C$ and $\delta^{18}O$) fractionation, supported by quantitative X-ray diffraction evidence, and whole-rock geochemical characterization of the Triassic Montney Formation indicates the presence of calcite, dolomite, magnesium, carbon and other elements. Results from isotopic signature obtained from bulk calcite and bulk dolomite from this study indicates depleted $\delta^{13}C_{PDB}$ (−2.18‰ to −8.46‰) and depleted $\delta^{18}O_{PDB}$ (−3.54‰ to −16.15‰), which is interpreted in relation to oxidation of organic matter during diagenesis. Diagenetic modification of dolomitized very fine-grained, silty-sandstone of the Montney Formation may have occurred in stages of progressive oxidation and reduction reactions involving chemical elements such as Fe, which manifest in mineral form as pyrite, particularly, during early burial diagenesis. Such mineralogical changes evident in this study from petrography and SEM, includes cementation, authigenic quartz overgrowth and mineral replacement involving calcite and dolomite, which are typical of diagenesis. High concentration of chemical elements in the Montney Formation -Ca and Mg indicates dolomitization. It is interpreted herein, that calcite may have been precipitated into the interstitial pore space of the intergranular matrix of very

fine-grained silty-sandstone of the Montney Formation as cement by a complex mechanism resulting in the interlocking of grains.

1. INTRODUCTION

The application of stable isotope geochemistry in the study of sedimentary rocks has increasingly become an integral part of sedimentary geology. In particular, isotopic composition of sediments is important in interpreting diagenesis resulting from dolomitazation, and differentiating sources of organic matter [1-3], classification of kerogen types [4], and correlating crude oils with source rocks [5-7]. [8] first originated and formulated the idea of using thermometer to measure the variations with temperature of fractionation factors in isotopic exchange equilibria, particularly, in relation to the oxygen isotopes in the system. Subsequently, [9] showcased that oxygen isotope ($\delta^{18}O$) in sedimentary carbonates can serve as a paleothermometer, and can be used to estimate the temperature at which carbonate was formed. The concept of using oxygen isotope as paleothermometer was developed on the premise that calcium carbonates precipitated by organisms is in isotopic equilibrium with the seawater in which the organisms grow [8-10].

This study of the Montney Formation in Fort St. John area (T86N, R23W and T74N, R13W), northeastern British Columbia (**Figure 1**) utilized stable isotopes (^{13}C and ^{18}O), whole-rock geochemistry (**Table 1**) and mineralogical composition (**Table 2**) to interpret dolomitization of the Montney Formation because they are established methods for studying dolomitization and diagenesis in carbonates [11, 12].

This research reported herein, primarily focus on using stable isotope ($\delta^{18}O$) to determine the paleotempeterature of precipitation of dolomite in the Triassic Montney Formation.

2. GEOLOGICAL SETTINGS

The Montney Formation is the basal stratigraphic unit of Triassic succession in the subsurface of western Canada [12-14]. It rests, unconformably in most areas, upon carbonate or mixed siliciclastic-carbonate strata of Carboniferous to Permian age [15-22]. The succession was deposited in a west-facing, arcuate extensional basin on the western margin of Pangaea [23-27]. The Montney Formation consists of siltstone, very fine-grained sandstone, bioclastic packstone/grainstone (coquina, in Alberta) [19, 20], interlaminated, interbedded, dolomitic silty-sandstone [12-14, 22] and shale. The Triassic Montney Formation is separated by an unconformity from the underlying Permian Belloy Formation (**Figure 2**).The unconformity along the Permian-Triassic boundary has been interpreted by [15, 20, 24] to be related to a global eustatic sea level fall. The global eustatic fall was related to the amalgamation of Pangaea Supercontinent, and was followed by a protracted Late Permian transgression that continued into the Triassic period [24]. The transgression was accompanied by anoxic conditions that induced profound environmental change [26-28], and may have severely increased levels of greenhouse gases [26-27]. These were the primary factors that contributed to the Late Permian-Triassic extinction crises, the largest extinction episode in geologic history [25, 27].

The paleoclimate reconstruction suggests that the paleoclimate may have ranged from sub-tropical to temperate [23-28]. The region has been interpreted to be arid during the Triassic, and was dominated by winds from the west [18, 28].

The WCSB forms a northeasterly tapering wedge of sedimentary rocks with thickness of more than 6000 meters, which extends southwest from the Canadian Shield into the Cordilleran foreland thrust belt [15, 29]. The Cordilleran of the WCSB provides the evidence that the origin and development of the basin was associated with tectonic activity [15, 30]. Later epeirogenic events resulted in subsidence that created the basin for sediment accumulation, which were attributed to the effects of contemporaneous episodes of orogenic deformation in the Cordillera [29, 31]; this is interpreted to be post Triassic, especially due to mountain influences [15].

Table 1. Whole-rock geochemistry showing Montney Formation chemical element concentrations. <DL means less than detection limit.

Well Location	Depth (m)	Major Elements								Trace Elements							
		Mg	Al	P	K	Ca	Ti	Fe	Mn	Li	Be	B	Co	Cu	Zn	V	Cr
		2	0.2	5	6	31	0.09	3.7	0.03	0.3	0.05	0.03	0.03	0.08	0.1	0.05	2
		ppm	ppm	ppm	ppm	ppm	ppm	ppm	ppm	ppm	ppm	ppm	ppm	ppm	ppm	ppm	ppm
b-39-H-93-p-9	2042	42,120	31,116	809	24,111	90,976	2795	16,707	297	26.9	51.9	39.1	18.3	43.1	1.2	51.4	<DL
d-39-F-93-p-9	2668.8	18,820	33,638	1246	24,251	71,508	3021	14,427	266	15	85.7	64.2	13.7	22.7	1.3	46.4	<DL
d-39-F-93-p-9	2685.4	13,338	40,861	2249	30,359	49,140	3668	20,717	253	17.3	77.7	42.5	23.5	89.6	1.4	62.8	<DL
d-39-F-93-p-9	2685.4	13,475	41,234	2289	30,453	48,968	3676	20,575	246	17.5	77.9	39	25	111	2	63	<DL
2-19-79-14W6	2048	19,780	45,633	1955	36,036	45,915	3877	19,687	253	21	288	26.7	24.1	33.8	1.8	69.3	<DL
2-19-79-14W6	2069.5	20,116	36,583	914	29,177	47,584	3397	16,679	332	17.9	530	28.7	19.1	221	1.5	61.2	<DL
2-19-79-14W6	2085	11,512	40,016	1493	32,310	36,429	3856	18,929	287	14.4	56.6	39.4	21.2	29.6	1.9	66.1	<DL
7-13-79-15W6	2055.22	48,152	24,438	1582	20,397	98,597	2080	22,999	364	21.8	271	27	30.5	24.6	1.1	70.1	<DL
7-13-79-15W6	2061.3	36,224	28,526	688	22,992	79,426	2704	14,057	355	12.7	55.2	40.5	15.2	28.3	1	52.4	<DL
7-13-79-15W6	2084.5	26,671	35,233	1717	27,941	61,980	3182	20,491	385	15.7	68.2	27.7	18.6	96.3	1.7	58.9	<DL
7-13-79-15W6	2101.78	14,456	39,659	2139	33,885	37,952	3576	26,134	324	12.4	78.5	58.7	29.3	270	2	65.7	<DL
9-29-79-14W6	1973	13,408	41,779	938	30,649	50,042	3938	16,527	296	15.6	504	45.1	19.2	82.3	1.6	68.2	<DL
9-29-79-14W6	1973	13,545	42,786	1003	31,695	51,007	3832	16,575	295	15.4	494	65.5	16.8	86.1	1.7	66.7	<DL
9-29-79-14W6	1999	11,761	36,736	2465	30,541	53,523	3347	15,951	331	11	46.9	28.1	18.1	68.7	1.1	49.9	<DL
GSP-2		**4993**	**61,382**	**1309**	**45,681**	**16,528**	**3521**	**27,936**	**288**		**46.4**	**9.41**	**38**	**121**	**1.3**	**19.8**	**<DL**
Certified value		**5800**	**78,800**	**1300**	**44,800**	**15,000**	**4000**	**34,300**	**320**	**36**	**52**	**7.3**	**43**	**120**	**1.5**	**20**	**-**
% recovery		**86.1**	**77.9**	**100.7**	**102**	**110.2**	**88**	**81.4**	**90**	**88.6**	**89.3**	**128.8**	**88.3**	**100.7**	**87.1**	**99.2**	**-**

Well Location	Depth (m)	Trace Elements															
		Ga	Ge	As	Se	Rb	Sr	Y	Zr	Nb	Mo	Ru	Pd	Ag	Cd	Sn	Sb
		0.01	0.02	0.06	0.2	0.04	0.03	0.02	0.09	0.04	0.02	0.01	0.01	0.01	0.06	0.06	0.01
		ppm	ppm	ppm	ppm	ppm	ppm	ppm	ppm	ppm	ppm	ppm	ppm	ppm	ppm	ppm	ppm
b-39-H-93-p-9	2042	8.36	1.13	10.9	1.64	77.9	279	23	178	9.22	1.95	0.26	7.86	0.53	0.08	3.39	0.95
d-39-F-93-p-9	2668.8	9.16	1.31	8.95	2.9	65	133	24	181	9.19	15.8	0.12	8.04	0.44	0.16	2.77	1.1
d-39-F-93-p-9	2685.4	12.2	1.43	17.7	3.53	88	121	28.3	256	11.9	13.8	0.03	11.1	0.59	1.11	3.35	1.17
d-39-F-93-p-9	2685.4	12.5	1.42	17.3	2.54	87.9	118	28.3	304	11.9	13.5	0.04	12.9	0.59	1.03	3.01	1.27
2-19-79-14W6	2048	14.5	1.6	19.9	3.06	96.8	107	28.4	172	11.7	28	<DL	7.31	0.5	0.34	3.32	3.55

Continued

2-19-79-14W6	2069.5	10.4	1.73	16.3	7.1	75.6	96.1	28.1	230	10.4	21.4	0.04	9.95	1.18	5.97	3.35	7.23
2-19-79-14W6	2085	11.2	1.63	8.01	2	81.3	100	28	281	12.7	4.98	<DL	11.7	0.55	0.28	2.95	0.63
7-13-79-15W6	2055.22	7.48	1.21	26	10.2	61.9	128	23.6	178	7.01	141	0.22	7.65	0.82	0.61	2.36	10.5
7-13-79-15W6	2061.3	6.83	1.17	7.84	2.71	53.6	111	22.7	195	8.99	28.7	0.23	9.21	0.44	0.35	3.02	0.91
7-13-79-15W6	2084.5	9.45	1.36	10.7	1.73	67.9	119	26.7	179	9.54	6.35	0.07	8.28	0.36	1.33	2.81	3.72
7-13-79-15W6	2101.78	11.3	1.55	15.6	2.11	79.3	107	29.4	241	11.8	70.1	<DL	11.1	0.79	6.03	3.1	2.16
9-29-79-14W6	1973	11.7	1.47	21	7.21	83.4	103	26.7	237	12.5	20.2	<DL	10.9	1.08	2.08	3.53	7.27
9-29-79-14W6	1973	12.6	1.41	22	9.26	85.5	103	26.5	230	11.8	21	<DL	10.6	1	2.07	3.23	7.1
9-29-79-14W6	1999	9.42	1.3	8.26	3.71	73.3	118	28.5	184	9.85	6.82	<DL	8.54	0.39	1.39	2.71	0.51
GSP-2		**22.3**	**1.92**	**2.14**	**4.54**	**269**	**245**	**24**	**400**	**22.2**	**2.15**	**<DL**	**18**	**0.61**	**0.16**	**7.99**	**0.36**
Certified value		**22**	-	-	-	**245**	**240**	**28**	**550**	**27**	**2.1**	-	-	-	-	-	-
% recovery		**101.2**	-	-	-	**109.9**	**102**	**85.8**	**72.7**	**82.4**	**102.2**	-	-	-	-	-	-

Well Location	Depth (m)	Rare Earth Elements (REE)										Trace Elements		
		Lu	Hf	Ta	W	Re	Os	Ir	Pt	Th	U	Au	Tl	Pb
		0.04	0.05	0.02	0.08	0.003	0.08	0.04	0.01	0.03	0.01	0.01	0.05	0.03
		ppm	ppm	ppm	ppm	ppm	ppm	ppm	ppm	ppm	ppm	ppm	ppm	ppm
b-39-H-93-p-9	2042	0.34	5.59	1.81	311	0.007	<DL	<DL	5.83	3.67	0.11	<DL	0.78	12.4
d-39-F-93-p-9	2668.8	0.36	5.73	1.76	996	0.026	<DL	<DL	4.26	4.89	0.1	<DL	1.88	12.5
d-39-F-93-p-9	2685.4	0.43	9.26	1.41	449	0.031	<DL	<DL	7.04	12.1	0.13	<DL	2.43	18.2
2-19-79-14W6	2048	0.41	5.32	1.16	236	0.022	<DL	<DL	5.61	6.24	0.09	<DL	2.97	15.6
2-19-79-14W6	2069.5	0.41	7.01	1.14	251	0.054	<DL	<DL	6.03	7.45	0.11	<DL	2.41	15.6
2-19-79-14W6	2085	0.44	8.61	1.49	490	0.017	<DL	<DL	6.26	5.16	0.13	<DL	1.18	17.1
7-13-79-15W6	2055.22	0.32	5.15	0.6	230	0.169	<DL	<DL	5.4	26.9	0.07	<DL	7.29	15.3
7-13-79-15W6	2061.3	0.37	6.94	1.69	363	0.007	<DL	<DL	6.87	5.91	0.12	<DL	1.56	8.11
7-13-79-15W6	2084.5	0.36	6.08	1.12	223	0.006	<DL	<DL	7.02	5.46	0.09	<DL	0.96	12.7
7-13-79-15W6	2101.78	0.41	7.99	1.69	507	0.092	<DL	<DL	6.69	13.1	0.12	<DL	8.2	24.1
9-29-79-14W6	1973	0.44	7.99	1.62	423	0.056	<DL	<DL	8.59	7.37	0.12	<DL	3.78	15.1
9-29-79-14W6	1999	0.37	6.1	1.05	312	0.021	<DL	<DL	4.32	6.51	0.07	<DL	1.03	15.3
GSP-2		**0.21**	**13.82**	**0.73**	**8.58**	**0.003**	**<DL**	**<DL**	**107**	**2.62**	**0.18**	**<DL**	**1.16**	**42.5**
Certified value		**0.23**	**14**	-	-	-	-	-	**105**	**2.4**	-	-	**1.1**	**42**
% recovery		**91.5**	**98.7**	-	-	-	-	-	**101.6**	**109.1**	-	-	**105.1**	**101.2**

Well Location	Depth (m)	Rare Earth Elements (REE)														
		Te	Cs	Ba	La	Ce	Pr	Nd	Sm	Eu	Gd	Tb	Dy	Ho	Er	Tm	Yb
		0.02	0.02	0.03	0.03	0.03	0.004	0.03	0.04	0.03	0.03	0.03	0.04	0.02	0.04	0.006	0.05
		ppm	ppm	ppm	ppm	ppm	ppm	ppm	ppm	ppm	ppm	pp	ppm	ppm	ppm	ppm	ppm
b-39-H-93-p-9	2042	<DL	3.88	219.63	25.48	42.06	5.96	23.48	4.96	1.14	4.94	0.66	4.11	0.85	2.41	0.35	2.27
d-39-F-93-p-9	2668.8	<DL	2.29	354.78	23.45	33.77	5.41	20.78	4.4	1.06	4.46	0.62	4.03	0.83	2.45	0.37	2.34
d-39-F-93-p-9	2685.4	<DL	3.7	345.98	30.04	42.3	6.6	25.25	5.29	1.17	5.24	0.74	4.81	1	2.96	0.44	2.81
d-39-F-93-p-9	2685.4	<DL	3.65	341.81	31.67	52.23	6.93	26.43	5.47	1.21	5.46	0.73	4.79	0.99	2.96	0.44	2.83
2-19-79-14W6	2048	<DL	4.16	380.24	31.14	44.5	6.51	24.91	5.03	1.27	5.16	0.7	4.79	0.99	2.85	0.42	2.8
2-19-79-14W6	2069.5	<DL	2.59	330.84	27.21	44.9	6.95	27.1	5.78	1.27	5.63	0.8	4.98	0.99	2.95	0.42	2.72
2-19-79-14W6	2085	<DL	2.64	334.07	29.93	43.85	6.62	24.77	5.08	1.12	5.02	0.7	4.75	1	2.96	0.43	2.9
7-13-79-15W6	2055.22	<DL	3.36	175.9	22.74	34.06	4.7	17.56	3.54	0.76	3.53	0.5	3.28	0.73	2.2	0.3	2.08
7-13-79-15W6	2061.3	<DL	1.99	265.11	24.52	46.27	5.88	22.09	4.48	1.03	4.52	0.64	4	0.83	2.45	0.36	2.33
7-13-79-15W6	2084.5	<DL	2.72	535.05	28.08	54.32	7.02	26.63	5.38	1.35	5.71	0.76	4.8	0.96	2.75	0.4	2.5
7-13-79-15W6	2101.78	<DL	2.8	339.91	32.6	46.42	6.78	25.18	5.12	1.18	5.26	0.75	4.71	0.99	2.9	0.42	2.77
9-29-79-14W6	1973	<DL	3.25	382.29	30.72	55.56	6.88	25.01	4.86	1.13	4.93	0.71	4.71	0.98	2.96	0.42	2.91
9-29-79-14W6	1999	<DL	2.32	532.15	28.13	36.39	6.45	25.39	5.21	1.28	5.44	0.74	4.87	1.01	2.84	0.4	2.63
GSP-2		**<DL**	**1.26**	**1190.09**	**186.53**	**407.31**	**54.36**	**198.84**	**26.06**	**2.63**	**15.62**	**1**	**5.67**	**0.96**	**2.64**	**0.28**	**1.75**
Certified value		**-**	**1.2**	**1340**	**180**	**410**	**51**	**200**	**27**	**2.3**	**12**	**-**	**6.1**	**1**	**2.2**	**0.29**	**1.6**
% recovery		**-**	**105.1**	**88.8**	**103.6**	**99.3**	**106.6**	**99.4**	**96.5**	**114.4**	**130.2**	**-**	**92.9**	**95.8**	**120.1**	**97.6**	**109.3**

Table 2. **Quantitative x-ray diffraction (XRD) analyses showing whole-rock mineralogy of the Montney Formation, British Columbia, Western Canada. Data source: B.C. Oil and Gas Commission.**

Depth (meters)	Formation	Quartz	K Feldspar	Plagioclase	Calcite	Dolomite	Pyrite	Marcasite	Apatite	Kerogen	Total Clay
2233.70	Montney	21.2	4.5	6	32.9	20.7	1.8	0	0	5.4	7.6
2236.40	Montney	15.2	5.2	2.1	52.9	9.8	1.1	0	2.8	8.1	2.9
2238.00	Montney	19.8	5.3	5	50	15.8	1.1	0	0	1.2	1.8
2240.80	Montney	19	4.8	3.4	25	20.3	2.5	0	0	17.6	7.3
2242.50	Montney	16.6	2.9	3.5	43.5	5.9	1.1	0	18.6	6.9	1
2245.60	Montney	23	4.5	5.2	36.1	8.2	2	0	6.5	8.7	5.8
2248.10	Montney	30.9	9.1	7.2	14.4	8.9	2.4	0	3.9	15.9	7.3
2251.50	Montney	24.4	5.5	5.4	31.9	7.7	2.2	0	2	11.3	9.6

Continued

2252.60	Montney	24	6.9	5.1	28.8	8.7	1.8	0.3	2.2	13.2	8.9
2259.50	Montney	33.6	13	9	10.7	14.7	1.2	0.6	2.5	11.7	3.1
2260.60	Montney	20.7	3.8	9.1	39.5	18.7	0.9	0	0	3.9	3.3
2262.00	Montney	22.9	6.7	9.5	43	10	1.2	0.6	0	1.5	4.7
2262.70	Montney	49	7.9	12.1	9.7	9.5	1.5	0.6	0	0	9.7
2265.20	Montney	20.6	4.7	7.3	53.1	6.2	1.2	0.3	0	2.4	4.4
2273.00	Montney	41.3	7.9	9.7	8.8	15.9	2	0.7	0.9	3.6	9.4
2279.20	Montney	34.6	9	10.9	9.9	17.4	1.6	0.5	0	6.3	9.8
2281.20	Montney	37.5	7.4	10.1	11.8	12.9	1.5	0.5	0	8.1	10.2
2282.40	Montney	39.9	7.8	9.9	10.4	9.8	1.8	0.4	1	9.1	10
2288.40	Montney	38.7	8.5	10.7	10.4	13.5	1.5	0.4	0	5.8	10.4
2294.60	Montney	44.9	7.9	13.6	9	12.6	1.4	0.4	0	0.1	10.2
2299.40	Montney	31.9	6.3	11.4	25.4	10.5	0.9	1	0	4.6	7.9
2317.80	Montney	33.3	7.1	9.9	2.9	33.1	1.1	0.7	0	2.6	9.4
2318.50	Montney	38.3	8.4	12.5	3	20.3	1.3	0.4	0	3.5	12.1
2323.90	Montney	37.8	7.8	12.5	3.4	21.4	1.2	0.4	0	4.5	11
2330.30	Montney	40.8	7.8	13.4	4.8	15.7	2.2	0.8	0	0.1	14.5
2332.80	Montney	31	6.5	8.6	4.7	31.7	1.5	0	0	6.8	9.2
2341.90	Montney	43.2	6.8	12.3	6.2	14.2	1.1	0.5	0	4.8	10.9
2352.39	Montney	22.5	3.5	8	13.7	41.5	1	0	0	3.4	6.3
2354.30	Montney	41	7.8	14.4	4.8	10.4	1.9	0.4	0	2.1	17.1
2355.94	Montney	42.4	7	10.5	5.3	13.4	1.4	0.4	0	5.3	14.3
2360.50	Montney	39.5	8.2	10.1	5.1	15.1	1.6	0.5	0	6.3	13.6
2366.00	Montney	43.4	6.7	13	6.3	9.8	1.6	0.4	0	5.5	13.2
2370.00	Montney	41	8.4	12.4	5.6	11.6	2.9	0.4	0	9.2	8.5
2370.60	Montney	38.5	9.9	11.2	4.9	11.8	3.2	0.4	0	11.4	8.7
2373.00	Montney	42.4	8.2	12.1	4.2	15.3	1.4	0.4	0	4.8	11.2
2377.00	Montney	22	3.5	6.8	27.6	31.6	0.6	0.3	0	3.1	4.4
2380.00	Montney	38.5	8.2	12.7	6.2	11.1	3	0.5	0	10.4	9.4
2383.15	Montney	34.2	6.3	9.2	4.3	27.6	2	0.3	0.3	6.9	8.8
2387.00	Montney	8.3	1.5	3.3	80.8	2.4	1.2	0	0	1	1.5
2390.20	Montney	45.8	6.7	14.6	4.3	11.4	2.1	0.6	0	0	14.5

Continued

2392.00	Montney	10.9	1.2	3.7	68.4	7.7	0.5	0.4	0	1.8	5.4
2394.30	Montney	8.1	1.1	3.2	78.2	6.8	0.6	0	0	0.5	1.6
2396.10	Montney	39.5	3.7	10.7	5.9	17.7	2.3	0.5	0	0	19.8
2400.00	Montney	40.4	4.5	13.8	4.6	12	1.9	0.6	0	3.7	18.4
2404.45	Montney	16.4	2.4	8.7	51	6.1	1	0.4	0	4	9.9
2415.70	Montney	31	3.3	7.7	5.2	23	2	0.8	0	3.1	23.8
2419.60	Montney	43	6.7	15.1	4.7	9.2	1.1	0.5	0	2.7	17
2421.80	Montney	41.4	5.5	12.3	3.6	10.3	1.4	1.1	0	4.1	20.4
2427.90	Montney	45.7	7.3	13.7	5.9	5.9	1.4	0.5	0	3.7	15.9
2428.70	Montney	42.3	3.6	13	8.6	6.2	2	0.6	0	4.6	19.1
2433.30	Montney	47.5	5.7	12.2	4.3	4	1.8	0.7	0	4.5	19.3
2435.40	Montney	43.4	5.3	11.8	4.9	6.2	1.7	0.7	0	4.2	21.8
2442.44	Montney	41.7	3.8	9.4	3.6	13.8	1.8	1.2	0	4	20.7
2447.76	Montney	46.2	5.5	10.8	2.2	4.6	2.2	0.6	0	5	22.9
2449.70	Montney	46.3	4	10.9	2.6	6	2.2	0.6	0	4.2	23
2453.90	Montney	42.7	4.6	10.7	3.5	6.4	2.1	0.6	0	4.5	24.8
2470.80	Montney	43.5	4.1	13	3.3	7	1.7	1.2	0	3.8	22.6
2481.70	Montney	43.5	4	9.3	3.5	7	1.8	1.1	0	5.1	24.8
2482.70	Montney	42.5	3.6	9.4	3.5	11	1.5	1.3	0	3.9	23.3
2486.00	Montney	41.6	3.8	10.5	3.6	7.2	1.7	1.3	0	3.7	26.6
2490.20	Montney	40	4.4	11.1	2.9	8	1.6	1.4	0	4.9	25.7
2492.70	Montney	38.7	4.1	9.7	3.1	16.2	1.7	1.1	0	3.2	22.1
2495.15	Montney	40.5	4.2	8.6	3.4	6.5	2.5	1.2	0	4.2	29
2501.65	Montney	44	2.8	8.7	3.7	6.5	1.9	0.8	0	5	26.6
2504.95	Montney	49.8	4.6	10	3.4	5.8	1.5	0.7	0.3	5.2	19.2
2506.15	Montney	25.1	1.2	4.1	2	54.1	0.6	0.6	0	2	10.3
2510.65	Montney	51.7	3.3	7.7	3.3	5.7	2	0.8	0	5.5	20
2512.55	Montney	47.8	4.3	8.4	3.3	5.4	2.2	0.7	0	5.7	22.1
2517.00	Montney	48.9	3.4	5.1	5.6	9	1.9	0.5	0	6.3	19.2
2522.70	Montney	49.1	3.1	4.4	3.9	6.6	2.5	0.8	0	6.7	22.9
2528.10	Montney	50	3.6	5.3	1	4.5	2.9	0.7	0	5.7	26.2
MINIMUM		**8.1**	**1.1**	**2.1**	**1**	**2.4**	**0.5**	**0**	**0**	**0**	**1**
MAXIMUM		**51.7**	**13**	**15.1**	**80.8**	**54.1**	**3.2**	**1.4**	**18.6**	**17.6**	**29**
AVERAGE		**35.7**	**5.5**	**9.4**	**15**	**12.9**	**1.7**	**0.5**	**0.6**	**5.1**	**13.6**

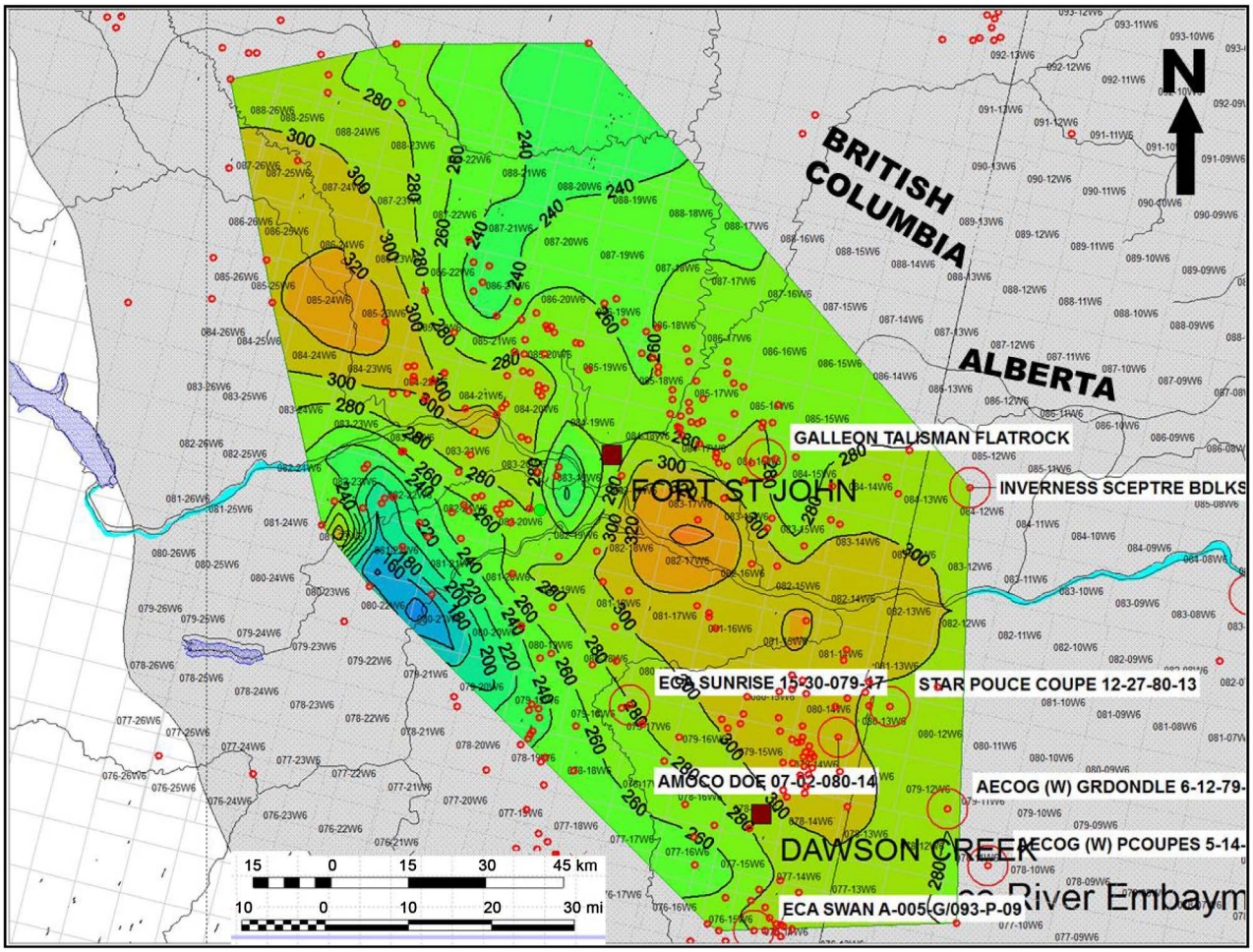

Figure 1. Location map of study area showing Montney Formation isopach contour map in northeastern British Columbia, Western Canada Sedimentary Basin (WCSB).

3. METHOD OF STUDY

The laboratory experiment and procedure for isotopic analyses in this study was performed in the isotope laboratory of Prof. Karlis Muehlenbachs in the Department of Earth and Atmospheric Sciences, University of Alberta (**Figure 3**). The extracted isotopic composition was analyzed using the Finnigan-MAT 252 Mass Spectrometer at the University of Alberta.

Stable isotope analysis for calcite and dolomite ($^{13}C/^{12}C$ and $^{18}O/^{16}O$) involves arrays of mechanics, namely;

1) Samples were grinded into uniform grains (powder form) using the pulverizing shatter box-machine for homogeneity of samples in order to provide a uniform surface area for acid reaction with samples following the method of [32], and samples were allowed to dry in air;

2) Samples were measured ~40 - 50 mg per sample and 3 ml of anhydrous phosphoric acid (H_3PO_4) were measured into each glass reaction vessel and evacuated overnight on a vacuum line to remove atmospheric components (gas) from the samples;

3) The samples were reacted with anhydrous phosphoric acid (H_3PO_4) at 25˚C for one hour. The reaction is expressed chemically as:

$$3CaCO_3 + 2H_3PO_4 \rightarrow 3H_2O + Ca_3(PO_4)_2$$

4) Following the method of [33], CO_2 was evolved after one-hour time from the reaction of acid with

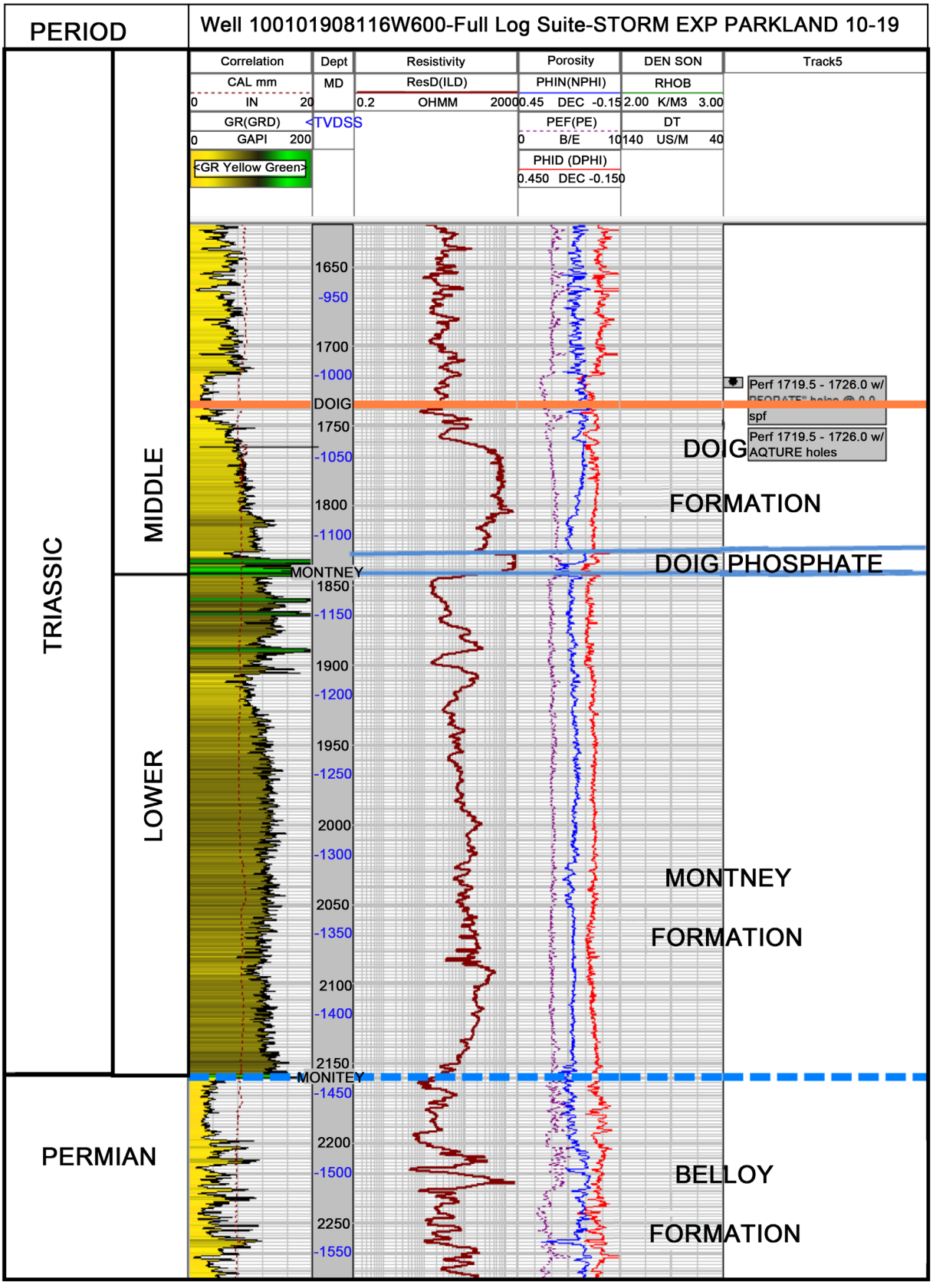

Figure 2. Type log of the Triassic Montney Formation [12], northeastern British Columbia, Canada.

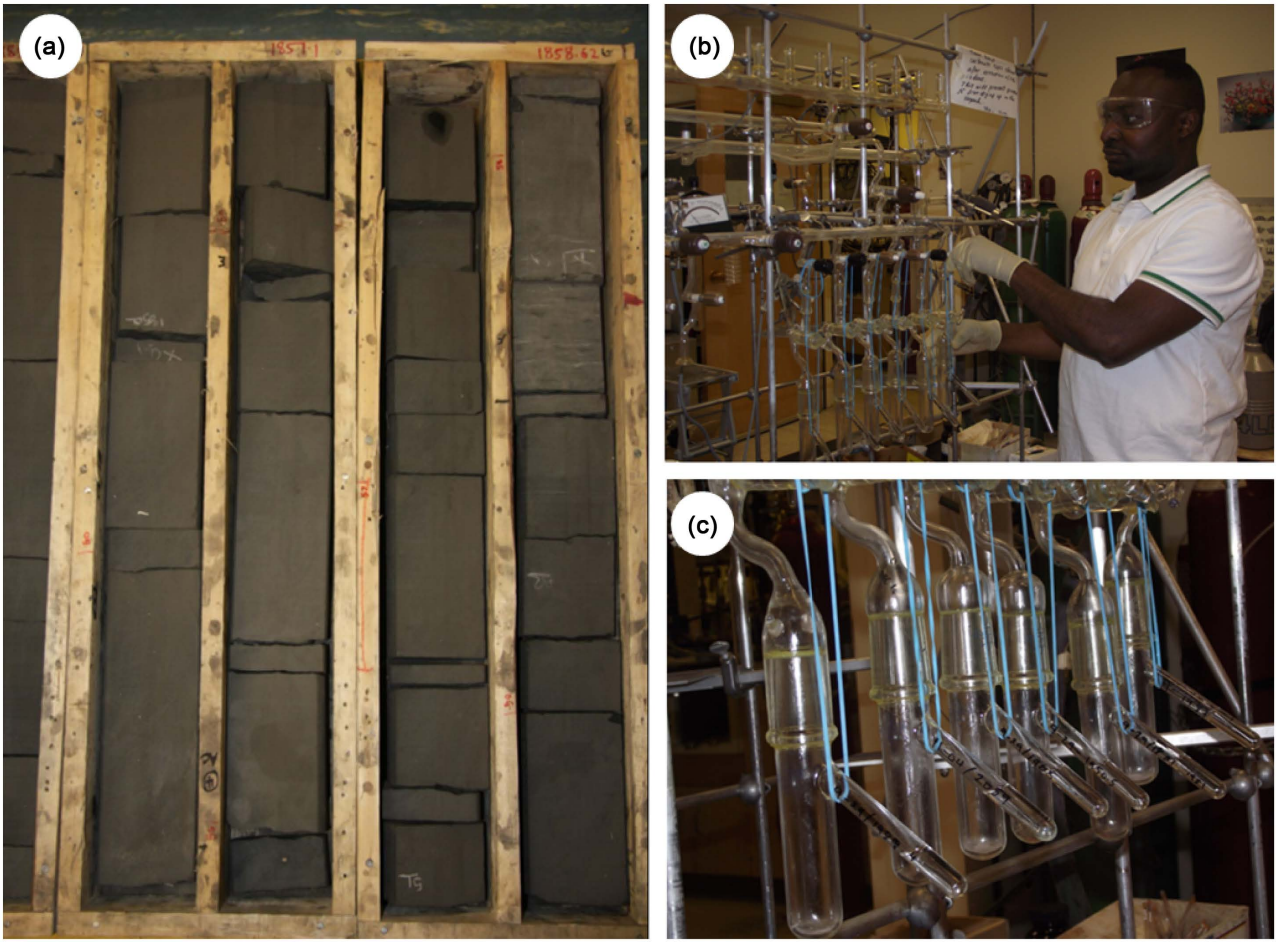

Figure 3. (a) Exemplifies Montney Formation core where samples were obtained for isotopes (^{13}C and ^{18}O) analyses; (b) Shows research scientist at the University of Alberta's Isotope Geochemistry Laboratory; loaded samples into glass reaction vessel to evacuate atmospheric components (gas) from the samples on a vacuum line; (c) Shows a magnified version of samples on a vacuum line from (b).

calcite in the sample;

5) This CO_2 was purified by distillation through a dry ice trap, condensed in a sample collection tube immersed in liquid nitrogen, and analyzed for calcite $\delta^{13}C$ and $\delta^{18}O$ values;

6) The CO_2 gas formed between the first and the fourth hour from the time of reaction was pumped out into a collection vessel as CO_2 for calcite to avoid contamination;

7) The vessel was then placed in a hot water bath at 25˚C and the reaction was left in that condition for 72 hours;

8) The CO_2 that formed during the remainder reaction was extracted in a similar process and analyzed for $\delta^{13}C$ and $\delta^{18}O$ of the dolomite component.

All analyses follow the standard method of [34]. The δ value is conventionally defined by [35], using the following expression:

$$\delta = \left(\frac{R_{\text{sample}}}{R_{\text{standard}}} - 1 \right) \times 1000 \quad (1)$$

where $R = {}^{13}C/{}^{12}C$ or ${}^{18}O/{}^{16}O$. The standard for carbonate is PDB [36], and that for water is SMOW [37]. The results derived from the analysis are shown in **Table 3**.

Table 3. Carbon and oxygen isotope data for bulk calcite cement and bulk dolomite analyzed from the Montney Formation, northeastern British Columbia, Canada.

Formation	Sample Location	Depth (m)	Bulk Calcite and Dolomite		
			$\delta^{13}C$ ‰ PDB	$\delta^{18}O$ ‰ PDB	$\delta^{18}O$ ‰ SMOW
Montney	9-29-79-14W6	1987.0	−5.07	−5.86	24.87
Montney	9-29-79-14W6	1989.0	−4.19	−16.15	24.66
Montney	9-29-79-14W6	2059.0	−5.08	−13.50	27.42
Montney	9-29-79-14W6	1981.0	−5.07	−5.86	24.87
Montney	9-29-79-14W6	1989.4	−3.70	−5.82	24.91
Montney	9-29-79-14W6	1983.0	−2.71	−5.51	25.33
Montney	9-29-79-14W6	1960.0	−2.87	−4.70	26.06
Montney	9-29-79-14W6	1987.0	−4.22	−7.19	23.58
Montney	9-29-79-14W6	1963.0	−4.22	−7.19	23.58
Montney	9-29-79-14W6	1987.0	−3.17	−5.39	25.35
Montney	11-04-79-14W6	2068.0	−3.83	−5.34	25.41
Montney	11-04-79-14W6	2074.0	−6.31	−3.66	27.14
Montney	11-04-79-14W6	1989.0	−4.10	−5.94	24.79
Montney	11-04-79-14W6	2068.0	−3.83	−5.34	25.41
Montney	11-04-79-14W6	2088.9	−8.46	−6.79	23.99
Montney	11-04-79-14W6	2059.0	−4.78	−3.54	27.67
Montney	11-04-79-14W6	1989.4	−2.78	−14.10	26.79
Montney	11-04-79-14W6	2091.0	−2.18	−3.66	27.14
Montney	D-39-F/93-P−9	2671.7	−2.18	−3.66	27.14
Montney	D-39-F/93-P-9	2668.0	−4.37	−8.17	22.48
Montney	7-13-79-15-W6	2055.3	−6.10	−5.84	24.9

4. RESULTS FROM THIS STUDY

4.1. Stable Isotope Geochemistry-Description of Data

Carbon and oxygen isotopes ($\delta^{13}C_{PDB}$ and $\delta^{18}O_{PDB}$) were analyzed in order to determine the bulk calcite and bulk dolomite ($\delta^{13}C$ and $\delta^{18}O$) isotopic signature of the Montney Formation (Table 3). The data in Table 3 and Figure 4 show in general, depletion in isotopic composition ($\delta^{13}C_{PDB}$ and $\delta^{18}O_{PDB}$) of both calcite and dolomite in the host lithology (very fine-grained silty-sandstone). The bulk calcite isotopic compositions of the Montney sediments range from ($\delta^{13}C_{PDB}$ −2.8‰ to −6.10‰, and $\delta^{18}O_{PDB}$ −3.66‰ to −16.15‰), and bulk dolomite isotopic composition values range from ($\delta^{13}C_{PDB}$ −2.71‰ to −8.46‰, and $\delta^{18}O_{PDB}$ −3.66‰ to −7.19‰) (Figure 4). High values (−13.50‰ to −16.15‰) occur in intervals that probably

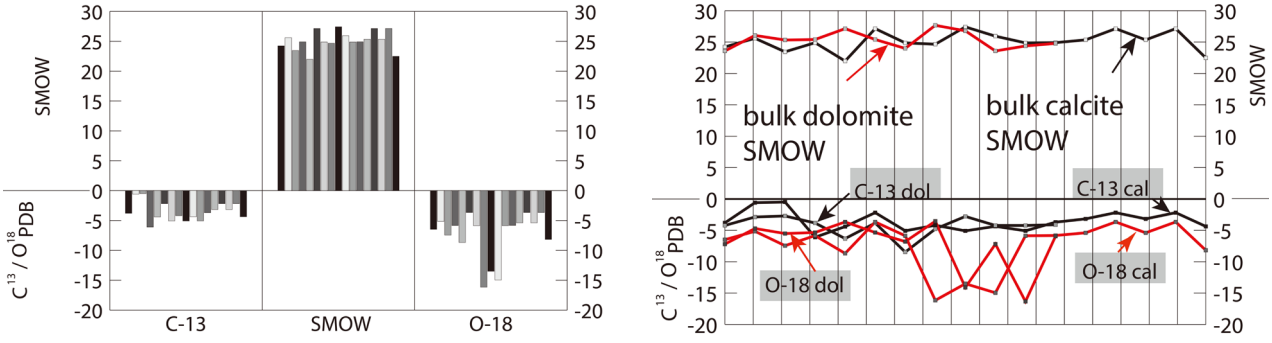

Figure 4. **Isotopic data plot for the Montney Formation. (a) Bar graph showing calculated $\delta^{13}C$, $\delta^{18}O$, and SMOW; (b) Displays $\delta^{13}C$, $\delta^{18}O$ (PDB) fields.**

have higher organic matter content or the presence of hydrocarbon. [36, 37] show that high negative $\delta^{13}{}_{PDB}$ depleted values greater than (−10) are associated with methane gas in the Formation. Within the study area, the high methane (gas) is probably the cause of high negative isotopic values (−13.50‰ to −16.15‰) seen in some of the analyzed samples from Montney Formation. According to a recent report by [38], in British Columbia, the Montney Formation host substantial hydrocarbon reserve with estimated volume of natural gas (271TCF), Liquified Natural Gas (LNG = 12,647 million barrels) and oil reserve (29 million barrels).

4.2. The Calculation of the Temperature of Fractionation of Calcite Was Rendered Using the Equation below [35]

$$10^3 \ln \alpha_{\text{Calcite-water}} = 2.78 \times 10^6 T^{-2} - 2.89 \tag{2}$$

There is a relationship:

$$10^3 \ln \alpha_{\text{Calcite-water}} \approx \delta^{18}\text{O}_{\text{calcite}} - \delta^{18}\text{O}_{\text{water}} \tag{3}$$

Therefore:

$$\delta^{18}\text{O}_{\text{calcite}} - \delta^{18}\text{O}_{\text{water}} = 2.78 \times 10^6 T^{-2} - 2.89 \tag{4}$$

Using the $\delta^{18}O_{PDB}$ range of bulk calcite (−2 to −7.19) assuming the $\delta^{18}O_{SMOW}$ value of pore water is between −2‰ and −7‰ (based on laboratory experiment from this study, which shows depleted $\delta^{18}O$ values; see **Table 3**).

The resultant expression by substituting into Equation (4) gives the following:

$$24.91(\text{SMOW})_{\text{calcite}} - (-2)\delta^{18} = 2.78 \times 10^6 T^{-2} - 2.89 \tag{5}$$

On solving Equation (5), gives:

$$T = 305.43 \text{ K}$$

The temperature in degrees Celsius (˚C) is 32.42˚C. Therefore, paleotemperature of precipitation of calcite during the Lower Triassic Period in the study area is ~32˚C.

4.3. For the Calculation of the Temperature of Fractionation of Dolomite, the Equation below Is Used [39]

$$10^3 \ln \alpha_{\text{Calcite-water}} = 3.2 \times 10^6 T^{-2} - 3.3 \tag{6}$$

Therefore:

$$\delta^{18}\mathrm{O}(\mathrm{SMOW})_{\mathrm{dolomite}} - \delta^{18}\mathrm{O}_{\mathrm{water}} = 3.2\times10^{6}T^{-2} - 3.3 \quad (7)$$

Using the δ^{18}O PDB range of bulk dolomite (−5 to −6.79) assuming the δ^{18}O (SMOW) value of pore water is between −5‰ and −7‰ (based on laboratory experiment which show a depleted δ^{18}O values).

By substituting into Equation (7), Equation (8) below is obtained:

$$23.99(\mathrm{SMOW}) - (-6.79)\delta^{18}\mathrm{O}_{\mathrm{water}} = 3.2\times10^{6}T^{-2} - 3.3 \quad (8)$$

The value of temperature T, which satisfies Equation (8) is: 306.4 K (33.3˚C). Therefore, $T = 33.3^{\circ}\mathrm{C}$ is the paleotemperature of precipitation of dolomite during the Lower Triassic Period in the present study. However, one of the samples analyzed in this study show paleotemperature of 13˚C.

4.4. Interpretation of Isotopic Signature

The values of the result from $\delta^{13}C_{PDB}$ bulk calcite (**Table 3**) show depletion in the isotopic composition ($\delta^{13}C_{PDB}$ −2.1‰ to −8.46‰). The negative $\delta^{13}C_{PDB}$ values are indicative of pore-water derived from seawater and dissolution of metastable carbonate in conjunction with organic matter decomposition by bacteria in sulfate reducing environment. The total organic carbon (TOC) of the Montney Formation is a result of high nutrient rich sediment source, rapid sedimentation, and preservation of organic matter [40] in oxygen-depleted, anoxic depositional environment [41-44]. This phenomenon explains the biasing of carbon isotope towards a very low (negative $\delta^{13}C_{PDB}$) discerned from the Montney Formation. The anoxic condition generate high alkalinity, which increases the total dissolved carbon that causes calcite to precipitate from pore-water, thereby biased towards light $\delta^{13}C_{PDB}$ values during early diagenesis [35].

The depleted $\delta^{18}O_{PDB}$ of bulk calcite values range from ($\delta^{18}O_{PDB}$ −3.54‰ to −16.15‰) and the $\delta^{18}O_{SMOW}$ range between 22.48‰ and 27.42‰ (**Table 3**, which is within the fresh water range) reported by [44] as indication of mixing of marine pore-water and meteoric groundwater during authigenic calcite precipitation. Applying the $\delta^{18}O_{PDB}$ range of the bulk calcite ($\delta^{18}O_{PDB}$ −3.54‰ to −16.15‰), the calcite fractionation equation $10^{3}\ln\alpha_{\text{calcite-water}} = 2.78\times10^{6}T^{-2} - 2.89$ [35, 44] and assuming that the $\delta^{18}O_{SMOW}$ values of pore-water is between −2 to −7.19, the paleotempertaure under which the calcite have precipitated is interpreted to have occurred between approximately 13˚C to ±33˚C (from analyzed samples; see calculation above). This interpretation is consistent with a warm paleotemperature reported for the Triassic period of western Canada [23, 45].

The bulk dolomite isotopic values ($\delta^{13}C_{PDB}$ −2.71‰ to −8.46‰) provide information on the origin and the precipitation of the dolomite. The very low (negative) values of $\delta^{13}C_{PDB}$ from the Montney sediment indicate depleted $\delta^{13}C_{PDB}$ (−2.71 to −8.46). The interpretation for the negative values (light bulk-dolomite $\delta^{13}C_{PDB}$) indicates that biogenic CO_2 significantly contributed to the total dissolved inorganic carbon [46]. The evidence of biogenic CO_2 contribution from isotopic signature is supported by the total organic carbon (TOC) content based on source-rock kerogen (**Table 2**) from the Montney Formation. The organic carbon content coupled with the depleted bulk dolomite ($\delta^{13}C_{PDB}$ −3.66‰ to −16.15‰) of the Montney Formation jointly indicate an anoxic, extremely poor oxidation environment where anaerobic sulfate reduction characteristic of early stage zone of methanogenesis occurs. The $\delta^{13}C_{PDB}$ has been used as a proxy of upwelling intensity because upwelling waters are ^{13}C depleted [11]. [47] assert that the upwelling isotopic effect might be compensated by the effect of planktonic blooms induced by the nutrient enrichment of upwelled water. The present of apatite mineral (**Table 2**) in the Montney Formation indicates upwelling of nutrient rich waters, which implies the presence of dissolved carbon in anaerobic condition.

The biasing towards light (warm) bulk dolomite $\delta^{18}O_{PDB}$ results show depleted in isotopic composition ($\delta^{18}O_{PDB}$ −2.71‰ to −8.46‰) indicates the present of meteoric water in the pore-water during precipitation of dolomite (Muehlembachs, 2011, personal communication). Further interpretation for the light, depleted isotopic values ($\delta^{18}O_{PDB}$ −2.71‰ to −8.46‰) suggest the formation within, or modification by meteoric water, or under elevated temperatures [38]. Applying the bulk calcite dolomite values of $\delta^{18}O_{PDB}$

−5.51‰ to −6.97‰, the dolomite-water fractionation equation $10^3 \ln\alpha_{\text{dolomite-water}} = 3.2 \times 10^6\ T^{-2} - 3.3$ [38], assuming the pore-water $\delta^{18}O_{SMOW}$ of −5.51‰ to −6.97‰, the dolomite was precipitated in temperatures ~33˚C. According to [48], oxygen isotopic analysis of marine carbonates gives at best, the estimate of temperatures at which the carbonate was deposited. The paleotemperature suggests that the Montney Formation has only encounter eodiagenetic realm of diagenetic stage.

On a geological time frame, the oxygen isotope composition of seawater is controlled by exchange of oxygen with silicate rocks [11, 49-51]. Unaltered silicate rocks are enriched in $\delta^{18}O$ relative to seawater by ~5.7‰ [11]. The isotopic composition of seawater is controlled by kinetic steady-states, reflecting major influxes of continental input, principally, the dissolved load of rivers; oceanic crust/seawater exchange at mid-oceanic ridges [52] and removal of chemical species via sedimentation [53].

High temperature interactions between seawater and rocks that occur during hydrothermal circulation are at axial mid-ocean ridges drive the isotopic composition of seawater towards increasing $\delta^{18}O$ that of the rock [50]. Low temperature interactions such as those that occur in off axis vent systems and during continental weathering, drive seawater isotopic composition towards low $\delta^{18}O$ [50], perhaps, such phenomenon may have implications for the low $\delta^{18}O$ values found in the Montney Formation.

5. DISCUSSIONS

5.1. Carbon and Oxygen Isotope Geochemistry

Important observation from isotopic studies of the Montney Formation sediments (very fine-grained, dolomitic silty-shale) shows that paleotemperatures of dolomitization is ~±33˚C. Such low temperature is characteristic of shallow burial, thus, suggests that the Montney Formation has only undergone eogenetic (early) phase of diagenesis and diagenetic process. The drive for warm temperature during the Triassic period have been reported to be associated with increase in CO_2 content in the atmosphere, which led to a global temperature increase that heralded most of the Permian-Triassic period [54].

The extraction of CO_2 during isotopic lab analyses for bulk calcite and bulk dolomite reveal that although the sediments are believed to be dolomitized, some of the analyzed samples show no evidence of calcite and in some cases, dolomite where not found (and therefore, not extracted). This observation was confirmed by utilizing X-ray diffraction (XRD) analyses, which explicitly confirms that dolomite and calcite where both found in most samples, but, in other samples, calcite was not present with dolomite and verse versa. Interpretation for this important discovery in the Montney Formation samples can be surmise in relation to the mode of substitution of Mg and Ca in carbonate rocks.

Thermodynamically, dolomite is stable in most natural solutions at earth surface conditions, and a thermodynamic drive exists for the conversion of calcite to dolomite [55]. Characteristically, most natural dolomite exhibits some degree of mixing of calcium and magnesium between cation layers [55, 56]. The phenomenon of the present/absent of calcite/dolomite in the Montney Formation proves that dolomites commonly depart from stoichiometric composition of an excess of calcium, which is accommodated in the magnesium layers [56, 57, 59]. Other explanations for the absent of calcite in some of the Montney Formation samples may be due to the fact that several cations, principally, Fe, Sr, Na, and Mn, substitute for calcite in many dolomites [58]. Significant amount of Fe, Sr, Na, and Mn in this study (**Figure 5**) support such possibility of substitution for calcite [58].

Overall, stable isotope geochemistry and results of this study leads to two important conclusions: 1) isotopic composition ($\delta^{13}C$ and $\delta^{18}O$) of the Montney Formation in the study area serves as a paleothermometer, and was used to constrain the temperature at which the carbonate (dolomite and calcite) associated with the Montney Formation was formed at seawater temperature ±33˚C. Mineral precipitation at low temperatures are enriched in ^{18}O while minerals formed at high temperatures show less ^{18}O enrichment [11]; and 2) dolomitized Montney Formation has mainly undergone eogenetic stage of diagenesis. The $\delta^{18}O\ SMOW_{\text{calcite}}$ values of (−3.66‰ to −16.15‰), and that of $\delta^{18}O_{\text{dolomite}}$ range from −2.71‰ to −8.46‰ indicate some oxidation of organic matter during diagenesis. This interpretation conforms with

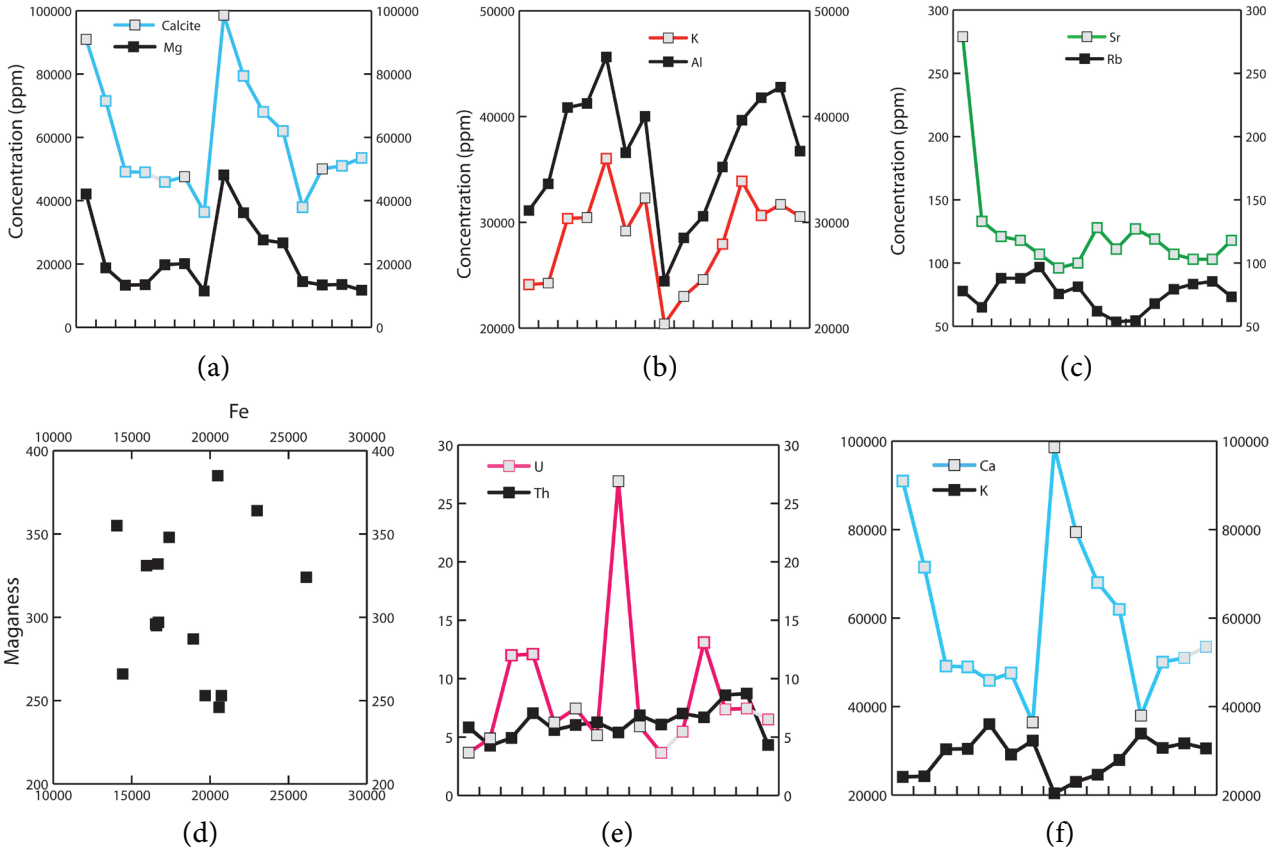

Figure 5. Shows the variation pattern of concentration of trace elements. (a) Illustrates the composition of dolomite, in which there is higher concentration of magnesium (Mg) relative to the calcite (Ca) component. The graph pattern shows good correlation between Mg and Ca; (b) Shows major elements, potassium (K) and aluminum (Al). The concentration of K is very high because of the clay mineral and the organic richness of the Montney Formation sediments. The Al concentration is related to the clay mineralogy and partly has affinity to organic matter. The graph pattern of K and Al correlates very well; (c) Shows alkaline earth metals—Strontium (Sr) and Rubidium (Rb) concentration; (d) Illustrates the concentration of Iron (Fe) and Manganese (Mn). Fe and Mn are both related to diagenesis. The concentration of Fe is very high compared to the concentration of Mn. This indicates that Fe has more dominating diagenetic influence in the Montney Formation. Evidence from thin-section petrography (Figure 6(d)) shows replacement of organic matter by pyrite; (e) Shows the relationship between radioactive elements—Uranium (U) and Thorium (Th). These elements are particularly related to the clay mineralogy and organic components of the Montney Formation sediments; (f) Shows the relationship between calcite (Ca) and Potassium (K). Evidently, Ca has enormously high concentration due to the stoichiometric co-existence with dolomite. Adapted from [12].

isotopic signature of depleted $\delta^{18}O_{SMOW}$ of [35] with respect to calcite-water fractionation equation, and dolomite-water fractionation of [38].

5.2. Dolomitization of the Montney Formation

Dolomite is a rhombohedra carbonate with the ideal formula $CaMg(CO_3)_2$, in which calcium and

magnesium occupy preferred sites [38]. [59, 60] used hydrothermal experiments extrapolated to low temperatures to demonstrate that calcite and dolomite are essentially ideal in composition at 25˚C. Thus, any double carbonate crystal of Ca and Mg at 25˚C is not essentially pure dolomite, and is either metastable or unstable with respect to calcite [38]. This relationship is evident in XRD analysis (**Table 2**), which supports the co-existence of dolomite and calcite.

Isotopic signature obtained from bulk calcite and dolomite results from this study indicates depleted ($\delta^{13}C_{PDB}$ −2.71‰ to −8.46‰) and ($\delta^{18}O_{PDB}$ −2.71‰ to −8.46‰), which is interpreted in relation to the oxidation of organic matter during diagenesis. Diagenetic modification of the very fine-grained, silty-sandstone of the Montney Formation may have occurred in stages of progressive oxidation and reduction reactions involving chemical element such as Fe, which manifest in mineral form as pyrite, particularly, during early burial diagenesis [61], or late stage diagenesis [62]. Mineralogical changes in the form of cementation and mineral replacement involving calcite and dolomite are typical of diagenesis [61], and are evident in the Montney Formation based on petrographic study and SEM.

Oxidation and reduction reaction mechanisms explains the modification of sediments, shortly after burial, prior to lithification or compaction during which fluids are ejected into the depositional interface [63, 64]. This phenomenon drives the oxidation and reduction processes involving Fe, sulfur, and carbon [61]. The significant amounts of organic matter (TOC) in the Montney Formation essentially make these elements principal reactants. The carbon compound of the organic matter content is the most rapidly oxidized and consequently contributing energy to drive the Fe into the ferrous state, thereby causing fixation of sulfur as pyrite [61]. Because of the present of organic matter in the Montney sediments, pyrite occurs as scattered "clots" in some of the samples examined. This occurrence is evident in thin-section petrography (**Figure 6**). Pyrite is related to post-depositional emplacement [65] caused by the dissolution of organic matter due to diagenesis.

High concentration of chemical elements in the Montney Formation, particularly, Ca and Mg indicate dolomitization. It is interpreted herein, that calcite may have been precipitated into the interstitial pore space of the intergranular matrix of the very fine-grained silty-sandstone of the Montney Formation as cement by a complex mechanism resulting in the interlocking of grains, welded together by calcite cement [66]. Evidence of grain interlocking is revealed by SEM image showing authigenic quartz overgrowth (**Figure 6**).

It is established through mineralogical composition in this study (**Table 2**) that the Montney Formation is quartz rich and contains clay minerals as well, including unstable mineral such as feldspar (**Table 2**). This sort of compositional mixture of quart, clay and feldspar minerals may have resulted in the decomposition of feldspar along the clay-quartz boundary due to processes involving hydrolysis in the course of diagenesis [61].

The depositional environment interpreted for the Montney Formation is proximal to distal offshore marine setting [14, 22]. In the marine environment, several weathering and transformation are prevalent. As a result, there exist an exchange of cations, in which the positions of clay minerals are changed, thereby resulting in the substitution of Mg for Ca [39, 40, 60]. In the marine environment chlorite and illite minerals are formed by fixation of Mg and K in montmorillonite or degraded illite delivered into distal settings due to continental denudation resulting from fluvial processes [40]. The present of illite and palygorskite clay mineral (**Figure 6**) support the evidence of diagenesis in the Montney Formation formed from ionic solutions in extreme conditions of temperature and pressure [40]. Dolomite in the Montney Formation appears as detrital in thin-section petrography (**Figure 7**). Such allogenic (non *in-situ*) dolomite and calcite may have only played a role (minimal) in the Montney Formation diagenesis, compared to sediments that are mainly composed of biogenic carbonate formed completely from aragonite and calcite [40]. Thus, authigenic calcite may have played dominant role in the vast diagenetic phenomenon in the Montney Formation.

6. CONCLUSIONS

Results obtained from isotopes (^{13}C and ^{18}O) from this study indicate depleted $\delta^{13}C_{PDB}$ (−2.71‰ to

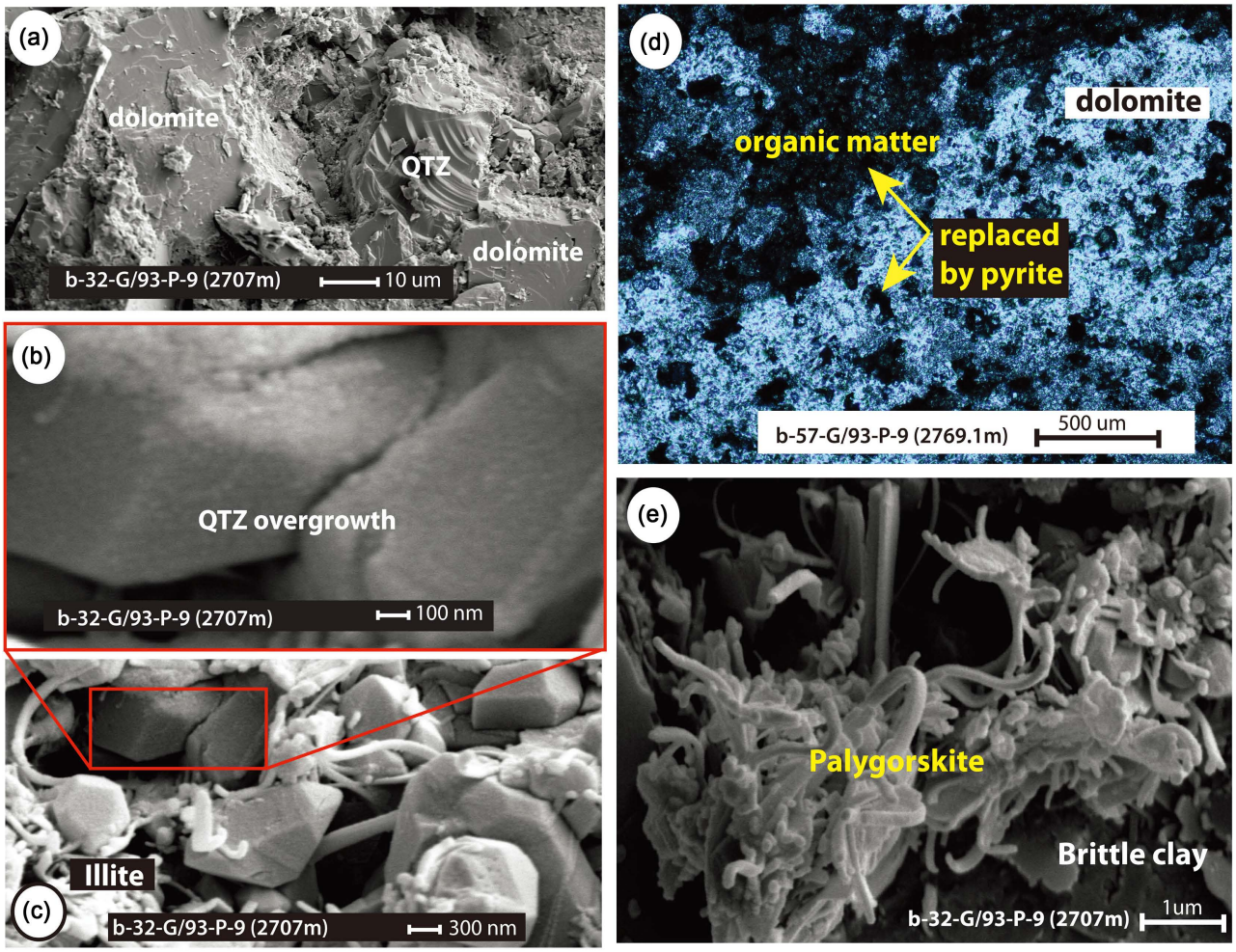

Figure 6. Microphotographs showing SEM and thin-section petrography of the Montney Formation illustrating the mineralogical composition. (a) Dolomite and quartz matrix. The quartz exhibits conchoidal fracture; (b) Shows magnification of plate C. Authigenic quartz overgrowth is illustrated in plate-B as evidence of grain dissolution due to diagenesis, and subsequent mineral precipitation (calcite) in the form of calcite cement that welded the grains together; (c) Shows quartz and illite with the authigenic quartz overgrowth; (d) Illustrates pyritized, dolomitized, organic carbon rich siltstone. Pyrite replaces organic matter in plate-D during decomposition of organic matter due to diagenensis; (e) Illustration of a very well formed palygorskite clay; a form of clay mineral growth, formed from the transformation of dickite to illite, and further transformation of illite to palygorskite due to severe temperature and pressure in a diagenetic regime. Adapted from [12].

−8.46‰) and it is related to oxidation of organic matter during diagenesis. Diagenetic modification of the Montney Formation (very fine-grained, silty-sandstone) may have occurred in stages of progressive oxidation and reduction reactions involving chemical element such as Fe, which manifest in mineral form as pyrite, particularly, during early burial diagenesis, or late stage diagenesis [67]. Mineralogical changes in the form of cementation and mineral replacement involving calcite and dolomite are typical of diagenesis. Based on isotopic signature and paleotemperature calculations, the calcite and dolomite of the Montney Formation may have formed at temperatures ranging from ~13˚C to ±33˚C, which is consistent with a warm, arid paleoclimate reported for the Triassic time [23, 30].

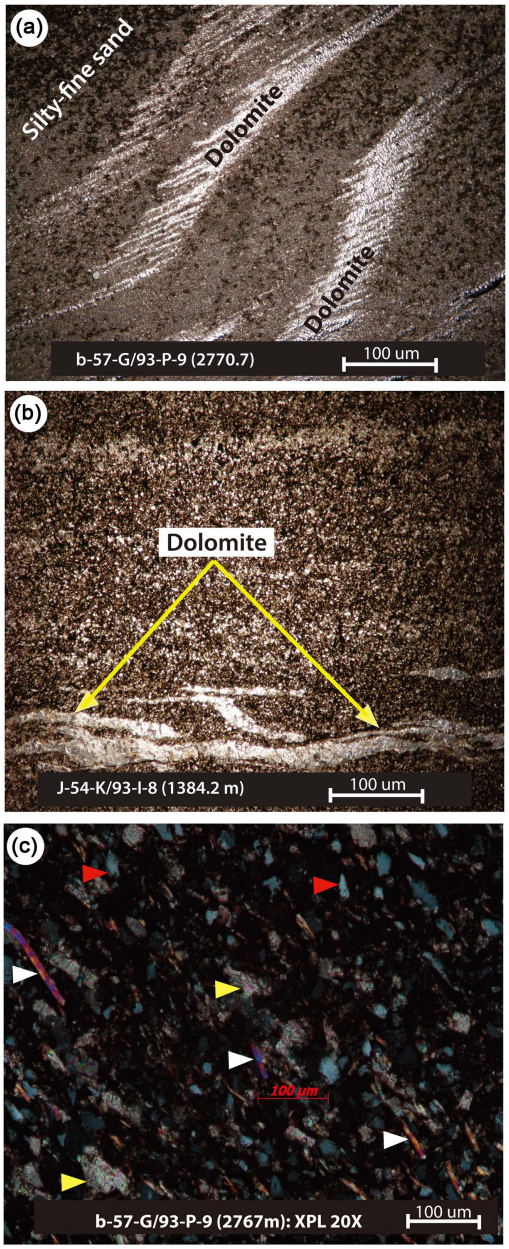

Figure 7. Photomicrographs showing dolomitic silty-sandstone. (a) Shows detrital dolomite resembles ripple; (b) shows detrital dolomite admixed siltstone [12]; (c) shows mica, quartz, dolomite, and detrital grains; red arrow = Quartz; yellow arrow = Dolomite; white arrow = Mica.

ACKNOWLEDGEMENT

Profoundly, I extend my appreciation to Professor Karlis Muehlenbachs for his mentorship and several stimulating discussions on carbonates and isotope geochemistry during the time I spent in his isotope lab at the University of Alberta. A big thank-you to Professors Murray Gingras and J-P Zonneveld for their support during my studies at the University of Alberta. The University of Alberta's Faculty of Graduate Studies and Research is greatly appreciated for awarding scholarship that supported this work. Laboratory Technician, Levner Olga is appreciated for all the support she offered during the lab work analyses.

Geoscience B.C. is highly appreciated for awarding scholarship in unconventional oil and gas reservoir research that supported this work in British Columbia. My thanks goes to Dr. Lucky Anetor for reviewing this manuscript and for his timely feedback.

REFERENCES

1. Sackett, W.M. and Thompson, R.R. (1963) Isotopic Organic Carbon Composition of Recent Continental Derived Clastic Sediments of Eastern Gulf Coast, Gulf of Mexico. *American Association of Petroleum Geologists Bulletin*, **47**, 525.
2. Hedges, J.I. and Parker, P.L. (1976) Land Derived Organic Matter in Surface Sediments from Gulf of Mexico. *Geochimica et Cosmochimica Acta*, **40**, 9.
3. Sturmer, D.H., Peters, K.E. and Kaplan, I.R. (1978) Source Indicators of Humic Substances and Proto-Kerogen: Stable Isotope Ratios, Elemental Composition, and Electron Spin Resonance Spectra. *Geochimica et Cosmochimica Acta*, **42**, 989-997.
4. Lewan, M.D. (1986) Stable Carbon Isotopes of Amorphous Kerogens from Phanerozoic Sedimentary Rocks. *Geochimica et Cosmochimica Acta*, **50**, 1583-1593.
5. Williams, J.A. (1974) Characterization of Oil Types in Williston Basin. *Bulletin of American Association of Petroleum Geologists*, **58**, 1243-1252.
6. Stahl, W.J. (1978) Source Rock-Crude Oil Correlation by Isotope Type-Curves. *Geochimica et Cosmochimica Acta*, **43**, 1573-1577.
7. Galimov, E.M. and Frick, M.G. (1985) Isotopic Method of Source-Rocks Diagnostic. *Geochemistry*, **10**, 1474-1486.
8. Urey, H. C. (1947) The thermodynamic properties of isotopic substances: Journal of the Chemical Society, 562-581. https://doi.org/10.1039/jr9470000562
9. Epstein, S., Buchsbaum, R., Lowenstam, H. and Urey, H.C. (1951) Carbonate Water Isotopic Temperature Scale. *Geological Society of America Bulletin*, **62**, 417-425. https://doi.org/10.1130/0016-7606(1951)62[417:CITS]2.0.CO;2
10. Burdige, D.J. (2006) Geochemistry of Marine Sediments. Princeton University Press, 609 p.
11. Killingley, J.S. and Berger, W.H. (1979) Stable Isotopes in a Mollusk Shell: Detection of Upwelling Events. *Science*, **205**, 186-188. https://doi.org/10.1126/science.205.4402.186
12. Egbobawaye, E.I. (2016) Whole-Rock Geochemistry and Mineralogy of Triassic Montney Formation, Northeastern British Columbia, Western Canada Sedimentary Basin. *International Journal of Geosciences*, **7**, 91-114. https://doi.org/10.4236/ijg.2016.71008
13. Egbobawaye, E.I., Zonneveld, J. and Gingras, M.K. (2010) Tight Gas Reservoir Evaluation in Montney and Lower Doig Formations, Northeastern British Columbia, Western Canada. *American Association of Petroleum Geologists Abstract*, **19**, 66-67.
14. Egbobawaye, E.I. (2016) Sedimentology and Ichnology of Upper Montney Formation Tight Gas Reservoir, Northeastern British Columbia, Western Canada Sedimentary Basin. *International Journal of Geosciences*, **7**, 1357-1411. https://doi.org/10.4236/ijg.2016.712099
15. Edwards, D.E., Barclay, J.E., Gibson, D.W., Kvill, G.E. and Halton, E. (1994) Triassic Strata of the Western Canada Sedimentary Basin. Geological Atlas of Western Canada (Chapter 16): Calgary, Canadian Society of Petroleum Geologists/Alberta Research Council, 257-275.
16. Podruski, J.A., Barclay, J.E., Hamblin, A.P., Lee, P.J., Osadetz, K.G., Procter, R.M. and Taylor, G.C. (1988) Conventional Oil Resources of Western Canada. Geological Survey of Canada Paper, 149 p.

17. Gibson, D.W. and Barclay, J.E. (1989) Middle Absaroka Sequence, the Triassic Stable Craton. In: Ricketts, B.D., Ed., *Western Canada Sedimentary Basin*: *A Case History*, Canadian Society of Petroleum Geologists, 219-231.

18. Zonneveld, J.P., MacNaughton, R.B., Utting, J., Beattty, T.W., Pemberton, S.G. and Henderson, C.M. (2010) Sedimentology and Ichnology of the Lower Triassic Montney Formation in the Pedigree-Ring/Border-Kahntah River Area, Northwestern Alberta and Northeastern British Columbia. *Bulletin of Canadian Society of Petroleum Geology*, **57**, 115-140. https://doi.org/10.2113/gscpgbull.58.2.115

19. Davies, G.R. (1997) The Triassic of the Western Canada Sedimentary Basin: Tectonic and Stratigraphic Framework, Paleogeography, Paleoclimate and Biota. *Bulletin of Canadian Petroleum Geology*, **45**, 434-460.

20. Orchard, M.J. and Tozer, E.T. (1997) Triassic Conodont Biochronology, Its Calibration with the Ammonoid Standard, and a Biostratigraphic Summary for Western Canada Sedimentary Basin. *Bulletin of Canadian Petroleum Geology*, **45**, 675-692.

21. Zonneveld, J.P., Gingras, M.K. and Pemberton, S.G. (2001) Trace Fossils Assemblages in a Middle Triassic Mixed Siliciclastic-Carbonate Marginal Marine Depositional System, British Columbia. *Palaeogeography*, *Palaeoclimatology*, *Palaeoecology*, **166**, 249-276.

22. Egbobawaye, E.I. (2013) Tight Gas Reservoir Characterization in Montney Formation, Northeastern British Columbia, Western Canada. Doctor of Philosophy Thesis, Department of Earth and Atmospheric Sciences, University of Alberta, Edmonton, 431 p.

23. Tozer, E.T. (1982) Marine Triassic Faunas of North America: Their Significance for Assessing Plate and Terrane Movements. *Geologische Rundschau*, **71**, 1077-1104. https://doi.org/10.1007/BF01821119

24. Henderson, C.M. (1997) Uppermost Permian Conodont and Permian-Triassic Boundary in the Western Canada Sedimentary Basin. *Bulletin of Canadian Petroleum Geology*, **45**, 693-707.

25. Zonneveld, J. (2011) Suspending the Rules: Unraveling the Ichnological Signature of the Lower Triassic Post-Extinction Recovery Interval. *Palaios*, **26**, 677-681. https://doi.org/10.2110/palo.2011.S06

26. Payne, J.L., Lehrmann, D.J., Wei, J., Orchard, M.J., Schrag, D. and Knoll, A.H. (2004) Large Perturbations of the Carbon Cycle during Recovery from the End-Permian Extinction. *Science*, **305**, 506-509. https://doi.org/10.1126/science.1097023

27. Kump, L.R., Pavlov, A. and Arthur, M.A. (2005) Massive Release of Hydrogen Sulfide to the Surface Ocean and Atmosphere during Intervals of Oceanic Anoxia. *Geology*, **33**, 397-400. https://doi.org/10.1130/G21295.1

28. Habicht, J.K.A. (1979) Paleoclimate, Paleomagnetism, and Continental Drift. American Association of Petroleum Geologists Studies in Geology, Vol. 9, 1-29.

29. Porter, J.W., Price, R.A. and McCrossan, R.G. (1982) The Western Canada Sedimentary Basin. *Philosophical Transactions of the Royal Society of London A*, **305**, 169-182. https://doi.org/10.1098/rsta.1982.0032

30. Price, R.A. (1994) Cordilleran Tectonics and the Evolution of the Western Canada Sedimentary Basin. In: Mossop, G.D. and Shetson, I., Eds., *Geological Atlas of the Western Canada Sedimentary Basin*, Canadian Society of Petroleum Geologists, 257-275.

31. Monger, J.W.H. and Price, R.A. (1979) Geodynamic Evolution of the Canadian Cordillera-Progress and Problems. *Canadian Journal of Earth Sciences*, **16**, 770-791. https://doi.org/10.1139/e79-069

32. Walters, L.J., Claypool, G.E. and Choquette, P.W. (1972) Reaction Rates and δ18O Variation for the Carbonate-Phosphoric Acid Preparation Method. *Geochimica et Cosmochimica Acta*, **36**, 129-140.

33. Epstein, S., Graf, D.L. and Degens, E.T. (1963) Oxygen Isotope Studies on the Origin of Dolomites. In: Craig, H., Miller, S.L. and Wasserburg, G.J., Eds., *Isotopic and Cosmogenic Chemistry*, North-Holland Publication Co., Amsterdam, 169-180.

34. McCrea, J.M. (1950) On the Isotopic Chemistry of Carbonates and Paleotemperature Scale. *Journal of Chemical Physics*, **18**, 849-857. https://doi.org/10.1063/1.1747785

35. Friedman, I. and O'Neil, J.R. (1977) Compilation of Stable Isotope Fractionation Factors of Geochemical Interest. U.S. Geol. Surv. Professional Paper 440-KK, Data of Geochemistry, 6th Edition, Chapter KK, KK1-KK12.

36. Craig, H. (1957) Isotopic Standards for Carbon and Oxygen and Correlation Factors for Mass-Spectrometric Analysis of Carbon Dioxide. *Geochimica et Cosmochimica Acta*, **12**, 2347-2349.

37. Craig, H. (1961) Standard for Reporting Concentrations of Deuterium and Oxygen-18 in Natural Waters. *Science*, **133**, 1833-1834. https://doi.org/10.1126/science.133.3467.1833

38. Sven Milelli (2013) New Report Doubles Previous Estimates of Montney Formation Natural Gas Reserves in British Columbia and Alberta. Canadian Energy Perspectives Publication. http://www.canadianenergylawblog.com/2013/11/14/new-report-doubles-previous-estimates-of-montney-formation-natural-gas-reserves-in-british%20columbia-and-alberta/

39. Land, L.S. (1983) The Application of Stable Isotopes to Studies of the Origin of Dolomite and Problems of Diagenesis of Clastic Sediments. In: Arthur, M.A., *et al.*, Eds., *Stable Isotope in Sedimentary Geology*, SEPM Short Course 10, 4.1-4.22.

40. Müller, G. (1967) Diagenesis in Argillaceous Sediments. In: Larsen, G. and Chilingar, G.V., Eds., *Diagenesis of Sediments*, Elsevier Publishing Co., New York, 128-177.

41. Demaison, G.J. and Moore, G.T. (1980) Anoxic Environments and Oil Source Rock Bed Genesis. *American Association of Petroleum Geologists Bulletin*, **64**, 1179-1209.

42. Ekdale, A.A. and Mason, T.R. (1988) Characteristic Trace-Fossil Associations in Oxygen-Poor Sedimentary Environments. *Geology*, **16**, 720-723. https://doi.org/10.1130/0091-7613(1988)016<0720:CTFAIO>2.3.CO;2

43. Bentley, S.J. and Nitouer, C.A. (1999) Physical and Biological Influences on the Formation of Sedimentary Fabric in an Oxygen-Restricted Depositional Environment: Eckernförde Bay, Southwestern Baltic Sea. *Palaios*, **14**, 585-600. https://doi.org/10.2307/3515315

44. Taylor, H.P.J.R. (1967) Oxygen Isotope Studies of Hydrothermal Mineral Deposits. In: Barnes, H.L., Eds., *Geochemistry of Hydrothermal Ore Deposits*: *Holt*, *Rinehart and Winston*, New York, 109-142.

45. Arnold, K.J. (1994) Origin and Distribution of Eolian Sandstones in the Triassic Charlie Lake Formation, Northeastern British Columbia. Unpublished M.Sc. Thesis, University of Alberta, Edmonton, 320 p.

46. Friedman, I. and Murata, K.J. (1979) Origin of Dolomite in Miocene Monterey Shale and Related Formations in the Temblor Range, California. *Geochimica et Cosmochimica Acta*, **43**, 1357-1365.

47. Bemis, B.E. and Geary, D.H. (1996) The Usefulness of Bivalve Stable Isotope Profiles as Environmental Indicators: Data from the Eastern Pacific Ocean and the Southern Caribbean Sea. *Palaios*, **11**, 328-339. https://doi.org/10.2307/3515243

48. Emiliani, C.M. (1954) Temperatures of Pacific Bottom Waters and Polar Superficial Waters during the Tertiary. *Science*, **119**, 853-855. https://doi.org/10.1126/science.119.3103.853

49. Muehlenbacks, K. and Clayton, R.N. (1976) Oxygen Isotope Composition of the Oceanic Crust and Its Bearing on Seawater. *Journal of Geophysical Research*, **81**, 4365-4369. https://doi.org/10.1029/JB081i023p04365

50. Muehlenbacks, K. (1998) The Oxygen Isotopic Composition of the Oceans, Sediments, and the Sea Floor. *Chemical Geology*, **86**, 263-273.

51. Perry, E.C., Ahmad, S.N. and Swulius, T.M. (1978) The Oxygen Isotope Composition of 2800 m.y. Old Metamorphosed Chert and Iron Formation from Isukasia, West Greenland. *Journal of Geology*, **86**, 223-239. https://doi.org/10.1086/649676

52. Quin, H. and Veizer, J. (1994) Oxygen and Carbon Isotopic Composition of Ordovician Brachiopods: Implications for Coeval Seawater. *Geochimica et Cosmochimica Acta*, **58**, 4429-4442.

53. Holland, H.D. (1984) The Chemical Evolution of the Atmosphere and Oceans. Princeton's Series in Geochemistry, Princeton University Press, Princeton, 582 p.

54. Wignall, P.B. and Hallam, A. (1992) Anoxia as a Cause of the Permian/Triassic Mass Extinction: Facies Evidence from Northern Italy and the Western United States. *Palaeogeography*, *Palaeoclimatology*, *Palaeoecology*, **93**, 21-46.

55. Morrow, D.W. (1990) Dolomite Part 1: The Geochemistry of Dolomitization and Dolomite Precipitation. In: Mcllreath, I.A. and Morrow, D.W., Eds., *Diagenesis*, Geoscience Canada Reprint, Vol. 4, 113-121.

56. Carpenter, A.B. (1980) The Chemistry of Dolomite Formation 1: The Stability of Dolomite. In: Zenger, D.H., Dunham, J.B. and Ethington, R.L., Eds., *Concepts and Models of Dolomitization*, Society of Economic Paleontologists and Mineralogists, Special Publication 28, 111-121. https://doi.org/10.2110/pec.80.28.0111

57. Goldsmith, J.R. and Graf, D.G. (1958) Structural and Compositional Variations in Some Natural Dolomites. *Journal of Geology*, **66**, 678-693. https://doi.org/10.1086/626547

58. Lumsden, D.N. and Chimahusky, J.S. (1980) Relationship between Dolomite Nonstoichiometry and Carbonate Facies Parameters. In: Zenger, D.H., Dunham, J.B. and Ethington, R.L., Eds., *Concepts and Models of Dolomitization*, Society of Economic Paleontologists and Mineralogists, Special Publication 28, 123-137. https://doi.org/10.2110/pec.80.28.0123

59. Veizer, J., Lemieux, J., Jones, B., Gilling, J.R. and Savelle, J. (1978) Paleosalinity and Dolomitization of a Lower Paleozoic Carbonate Sequence, Somerset and Prince of Wales Island, Arctic Canada. *Canadian Journal of Earth Sciences*, **15**, 1448-1461. https://doi.org/10.1139/e78-151

60. Graf, D.L. and Goldsmith, J.R. (1956) Some Hydrothermal Syntheses of Dolomite and Protodolomite. *Journal of Geology*, **64**, 173-186. https://doi.org/10.1086/626332

61. Goldsmith, J.R. and Heard, C.D. (1961) Subsolidus Phase Relations in the System CaCO3-MgCO3. *Journal of Geology*, **69**, 45-74. https://doi.org/10.1086/626715

62. Dapples, E.C. (1967) Diagenesis in Sandstones. In: Larsen, G. and Chilingar, G.V., Eds., *Diagenesis of Sediments*, Elsevier Publishing Co., New York, 91-125.

63. Degens, E.T. (1967) Diagenesis of Organic Matter. In: Larsen, G. and Chilingar, G.V., Eds., *Diagenesis of Sediments*, Elsevier Publishing Co., New York, 343-390.

64. Weller, J.M. (1959) Compaction, of Sediments. *American Association of Petroleum Geologists*, **43**, 273-310.

65. Von Engelhardt, W. and Gaida, K.H. (1963) Concentration Changes of Pore Solutions during the Compaction of Clay Sediments. *Journal of Sedimentary Petrography*, **33**, 919-930. https://doi.org/10.1306/74D70F74-2B21-11D7-8648000102C1865D

66. England, G.L., Rasmussen, B., Krapez, B. and Groves, D.I. (2002) Palaeoenvironmental Significance of Rounded Pyrite in Siliciclastic Sequences of the Late Archean Witwatersrand Basin: Oxygen-Deficient Atmosphere or Hydrothermal Alteration? *International Association of Sedimentologists*, **49**, 1133-1156.

67. Waldschmidt, W.A. (1941) Cementing Materials in Sandstones and Their Probable Influence on the Migration and Accumulation of Oil and Gas. *American Association of Petroleum Geologists Bulletin*, **25**, 1839-1879. https://doi.org/10.1306/3D9333F6-16B1-11D7-8645000102C1865D